

# Conductive Polymer Composite Materials and Their Utility in Electromagnetic Shielding Applications

Richard T. Fox,<sup>1</sup> Vijay Wani,<sup>2</sup> Kevin E. Howard,<sup>3</sup> Andrew Bogle,<sup>4</sup> Leo Kempel<sup>4</sup>

<sup>1</sup>The Dow Chemical Company; Plastics—Dow Building Solutions, The Dow Chemical Co., Midland, Michigan

<sup>2</sup>The Dow Chemical Company; Plastics—Materials Research, The Dow Chemical Co., Freeport, Texas

<sup>3</sup>The Dow Chemical Company; New Products R&D, Core R&D, The Dow Chemical Co., Midland, Michigan

<sup>4</sup>Department of Electrical and Computer Engineering, The Michigan State University, East Lansing, Michigan

Received 10 May 2007; accepted 10 July 2007

DOI 10.1002/app.27317

Published online 13 November 2007 in Wiley InterScience (www.interscience.wiley.com).

**ABSTRACT:** Commercial electronic devices require shielding solutions that ensure electromagnetic compatibility (EMC) while accounting for effects of specific enclosure structural features such as seams, vents, and port dimensions. In practice, suitable EMC materials combine with the device operating characteristics to determine an overall shielding response. To optimally couple plastic design practices with EMC requirements, both polymer materials science and electrical engineering concepts, must be considered. Use of extrinsically conductive polymer (ECP) formulations for electronic applications has advantages in that they can be directly molded to a desired shape and serve to provide the necessary shielding while also meeting mechanical integrity requirements. Shielding and mechanical performance can be varied via filler loading or altered through wall thickness changes to satisfy demands

associated with a particular device. Injection-moldable ECP polycarbonate-based formulations can attain average shielding effectiveness (SE) levels of ~50–60 dB through 2 GHz at 2-mm thickness as measured using ASTM D 4935 procedures. These values vary with thickness, and SE improvements of ~10–20 dB are observed when increasing from 1 to 2 mm. Additionally, resultant mechanical properties of shielding composites are strong functions of overall fiber content. These interrelated material and shielding characteristics, which form the basis for filled conductive polymer use within practical enclosure shielding designs, are described. © 2007 Wiley Periodicals, Inc. *J Appl Polym Sci* 107: 2558–2566, 2008

**Key words:** composites; compounding; conducting polymers; fibers; fillers; injection molding

## INTRODUCTION

Commercial electronic enclosure designs require shielding solutions, which retain not only mechanical integrity, but also account for the effects of structural characteristics such as wall thickness, seams, and slot opening dimensions on emission control. Although planar walls shield well against progressively higher frequencies, specific design of aperture/seam features is dependent upon the emission source and its generated signal spectrum. Consequently, the operating characteristics of the integrated circuits (ICs) making up the device functions add to overall enclosure design considerations.

Extrinsically conductive polymer (ECP) formulations<sup>1–7</sup> within electronic applications are useful in that they can be directly molded to the desired shape and serve as both the structural material and the shield. Performance can be varied via filler loading to satisfy requirements dictated by the specific device demands or accommodated through localized

wall thickness changes. Understanding both the capabilities and limitations of their use in practice is of importance to designers.

As background on shielding behavior, dynamic electromagnetic waves have coupled electric (E) and magnetic (H) field components. Materials are traditionally described in terms of several bulk property quantities: permeability ( $\mu$ ), permittivity ( $\epsilon$ ), and conductivity ( $\sigma$ ). These intrinsic properties of shielding materials influence overall attenuation of the propagating wave and in general are dispersive. Electromagnetic interference (EMI) issues for portable electronic systems are concerned primarily with E-field shields because H-fields are typically more prominent in high-current devices. Numerous literature sources<sup>8–16</sup> describe the theoretical basis for shielding performance. The primary shielding mode of such materials is reflection, though in some cases absorption also plays a role.

The shielding effectiveness (SE) of a material is the ratio of the incident field strength (V/m) to that fraction, which is transmitted, expressed in a decibel scale as  $20 \log_{10} (E_i/E_t)$  (dB). Total SE is the sum of three parts: reflection, absorption, and rereflection.<sup>17</sup>

Correspondence to: K. Howard (kevinehoward@dow.com.).

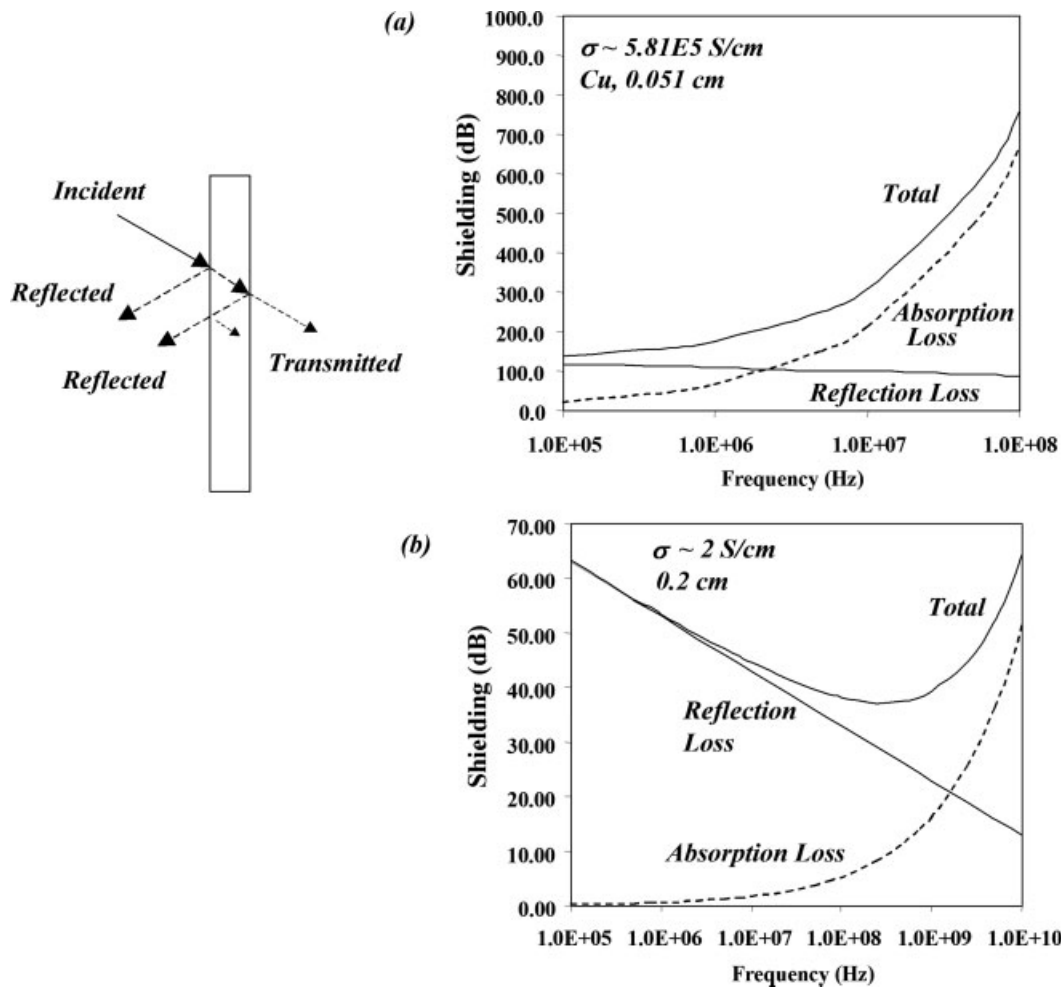


**Figure 1** Theoretical shielding levels (dB) with respect to frequency for (a) a highly conductive material such as copper (~ 0.020 in) and (b) performance of a lower conductivity material with four times the copper thickness.

$$SE_{dB} = R_{dB} + A_{dB} + B_{dB}$$

where  $R_{dB}$  is the shielding due to reflection,  $A_{dB}$  the shielding due to absorption, and  $B_{dB}$  the shielding due to rereflection.

Fields impinging on a material with different characteristic impedance than the media it was propagating in (usually free-space) will partially transmit and partially reflect. Rereflection (also known as multiple reflections) is due to one or more reflections within the material and is typically ignored if the reflection term ( $R_{dB}$ ) or absorption term ( $A_{dB}$ ) are dominant. In the present instance, ( $B_{dB}$ ) will be assumed to be negligible and therefore ignored. Figure 1 illustrates the physical scenario and quantifies reflection and absorption contributions to the SE.

In this figure, the SE of copper (a very good conductor) is compared to a lower conductivity material that is four times the thickness of the copper. As can be seen, the copper is an excellent, though expensive, shielding material from 100 kHz through 100 MHz. However, sufficient shielding performance

can be achieved by a less conductive material, such as ECP, if sufficient thickness is used in the construction of the enclosure.

Digital circuits generate substantial noise levels throughout a wide frequency spectrum and can serve as a source of EMI. For example, the content of a typical square wave contains contributions from both the clock rate and the edge rate (or rise time) of the waveform. The highest spectral component of this signal is attributed to the rising transition (e.g., rise time from low to high state), and consequently, it is this contribution, which typically impacts electromagnetic compatibility (EMC) product compliance.

The amplitude diminishes as shown in Figure 2 depending upon the waveform characteristics.<sup>14-16</sup> Figure 2 lists some typical example clock rate and rise time values to demonstrate effects on generated emissions, and consequently, shielding requirements may be significant at higher frequencies.

Shielding design for emissions at these high frequencies can be difficult, because apertures within

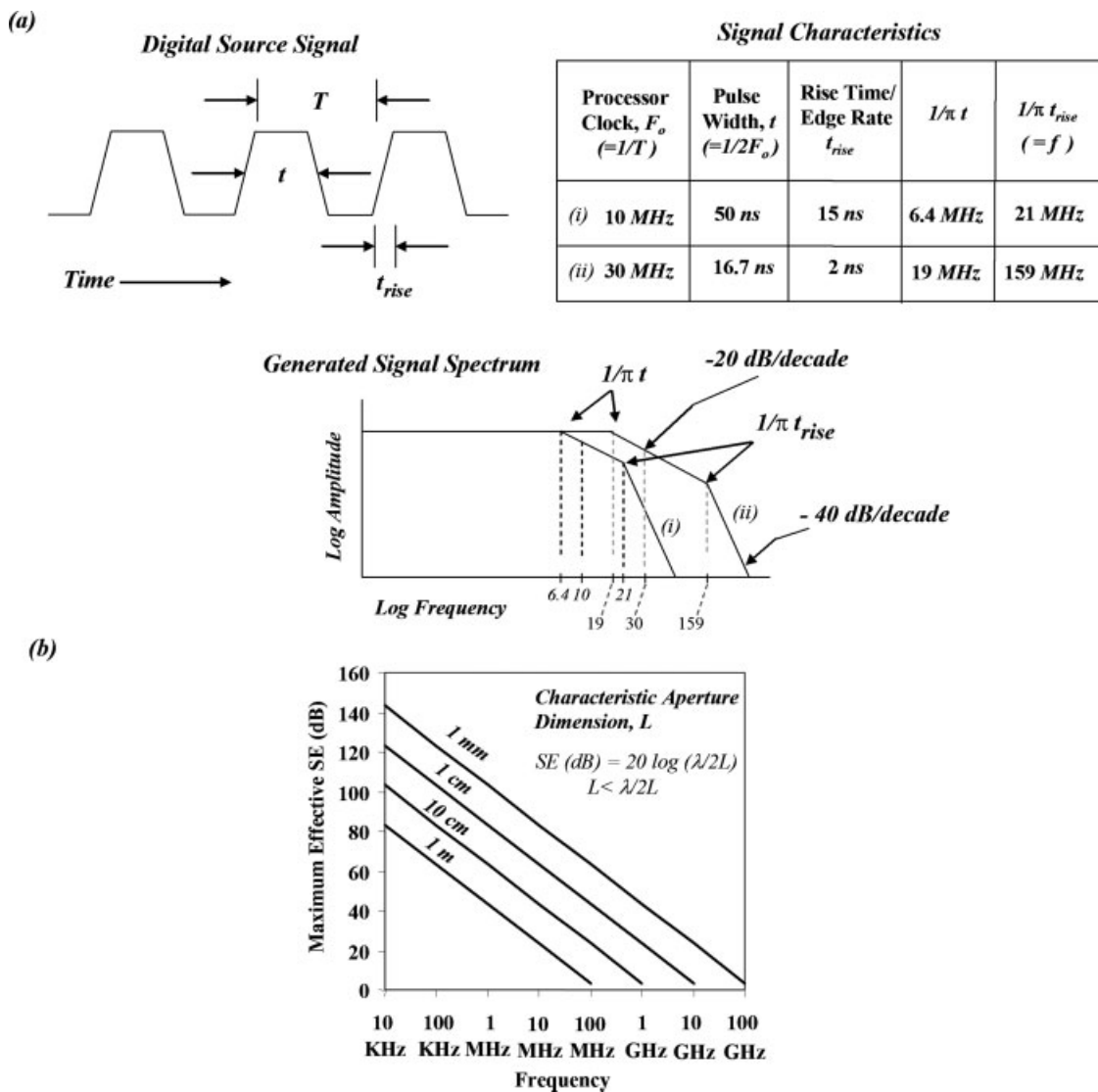


**Figure 2** Clock rates and rise time example effects on radiated emission characteristics.<sup>14</sup> (a) A representative typical digital signal with respect to time and its corresponding spectrum in the frequency domain is shown. Shielding strategies must account for frequency content which can be significantly higher than the actual operating frequency. (b) Relationship for attenuation in the vicinity of an enclosure aperture such as a seam, slot or hole. Design rules of thumb suggest maintaining characteristic dimensions  $\leq \lambda/20$ , and preferably  $\leq \lambda/50$  for the upper frequencies of concern.

the enclosure impact overall SE as shown in Figure 2(b). Opening dimensions exceeding  $\lambda/2$  provide no emission attenuation, and as a result, the influence of the inherent capability of the shield can be minimized. Consequently, both material characteristics and aperture dimensions combine to determine overall shielding response in practice.

Material characteristics, specific enclosure features, and overall shielding requirements are then interrelated considerations within operational electronic enclosures. The objective of this work is to describe group of practical conductive composite materials, which can be utilized for these applications. This includes extrinsically conductive composite formulations, which can combine various fibrous filler types to capitalize on the mechanical and electrical proper-

ties of metal and metallized fiber characteristics. Representative mechanical, electrical, and shielding properties are evaluated with respect to formulation detail, offering a guide for material selection within particular enclosure designs.

## EXPERIMENTAL

Polycarbonates with melt flow rates between 15 and 22 were used as a base resin.<sup>18</sup> Stainless steel<sup>19</sup> and nickel-carbon<sup>20</sup> long fiber tows suitable for injection molding and encapsulated in polycarbonate at  $\sim 0.50$ – $0.60$  weight fiber within the tows were utilized and are illustrated in Figure 3. Fibers form a conductive network within the molded composite,

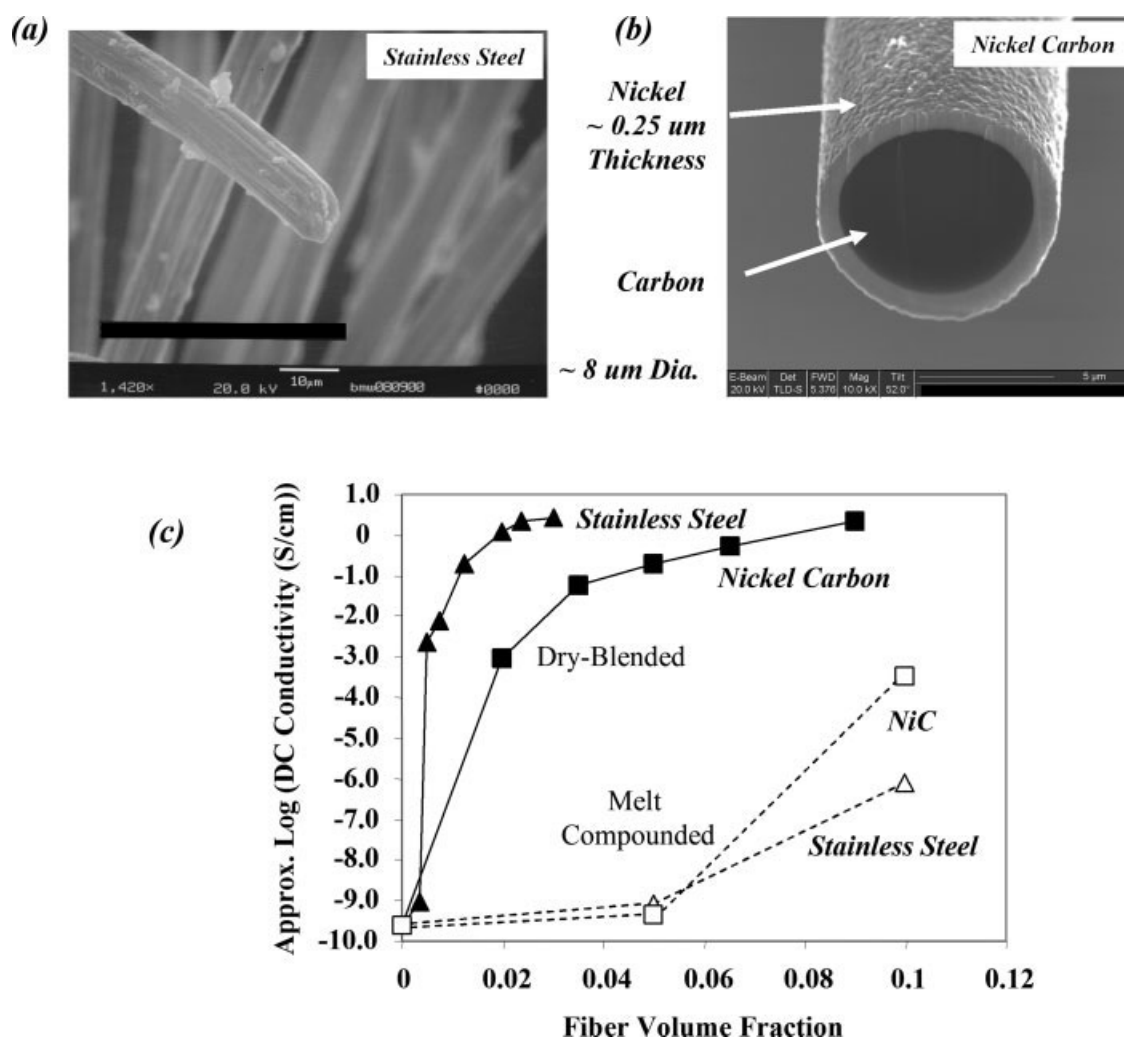


**Figure 3** Fibrous fillers utilized within ECP composites. Scanning electron micrographs of as-received (a) stainless steel and (b) nickel-carbon (NiC), both at 8- $\mu\text{m}$  diameters. (c) Influence of the processing method on volumetric DC conductivity of resultant molded composites. Note that measured DC conductivity here is only approximate at low levels, exceeding instrument range.

which then acts as the shielding barrier against electromagnetic energy passage. Typical-molded composites are processed via melt compounding the desired additives with a polymer to form a concentrate pellet, followed by injection molding of the desired article. Mechanical work input during polymer melting and the shear conditions encountered during compounding can lead to fiber attrition in reinforced composites and would be anticipated to affect composite volumetric DC conductivity. Consequently, conventional melt compounding to intimately preblend the fibers within the matrix into a pellet is not used. Rather, fiber tow concentrates are dry blended with the polymer and then added directly in the molding machine hopper. A Battenfeld 22-ton-molding machine with a 14 : 1 L/D screw was used. Figure 3 illustrates that the impact of processing route on resultant percolated conductivity

is considerable and can lead to electrical performances, which differ by several orders of magnitude.

Optical characterization of processed fiber was performed by dissolving molded parts within a solvent and then measuring individual fiber lengths under a stereoscope equipped with digital image analysis capability. Figure 4 reveals significant resultant aspect ratio differences between processing routes. Stainless fibers retain longer overall lengths than NiC due to greater ductility and toughness, consequently forming more entangled and efficient networks from a conductivity perspective. Relative morphology differences with NiC fibers are also illustrated in Figure 4; NiC is brittle and more readily breaks into smaller lengths, which does not degrade flow characteristics to the same extent as stainless steel. As a result, mixtures of the two types are preferred from a combined forming and shielding perspective.

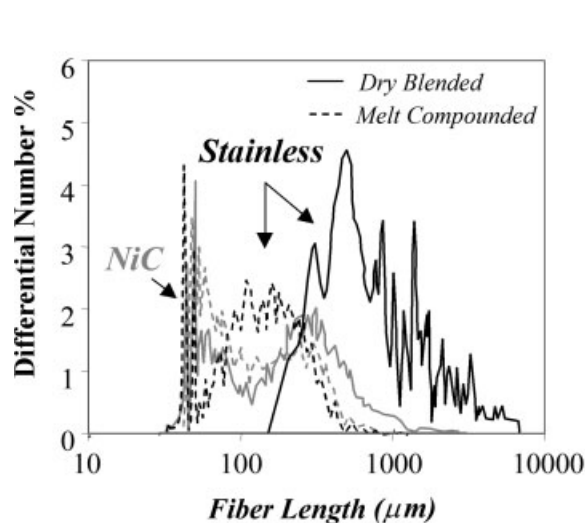


**Figure 4** Fiber length distributions and aspect ratios following differing processing routes. Relative fiber morphology characteristics contrasted in micrographs.

SE of planar materials is typically measured as specified by ASTM D 4935-99<sup>21</sup> over a frequency range from 30 MHz to 1.5 GHz. An Electro-Metrics Model EM-2107A SE test fixture was used with an Agilent E8361A Vector Network Analyzer to measure 13.3-cm circular diameter specimens at the desired wall thickness. These were molded using a Krauss Maffei 110-ton machine with a 23 : 1 L/D screw. Alternatively, SE can be measured via Stripline Field techniques.<sup>22</sup>

## RESULTS AND DISCUSSION

Discontinuous filler composite volumetric DC conductivity is typically considered in conjunction with percolation theory,<sup>23-28</sup> in which a threshold loading induces an abrupt change in a given physical property. This level is filler-geometry dependent and has been applied to describe electrical/thermal conductivity, viscosity, dielectric constant, and modulus observations within various composites. In this instance, the network of conducting linkages reaches a threshold concentration in which the molded part transitions from an insulator to a conductor and can be predicted<sup>29</sup> based upon both aspect ratio and loading fraction as shown in Figure 5.

Figure 6 suggests that the percolation volumetric threshold values observed within molded compositions are in reasonable agreement to those predicted values, although measured conductivity magnitudes beyond this level are lower than theoretical projections. Measured DC conductivity is a combined function of intrinsic filler conductivity, loading level, fiber geometry, and also potentially influenced by contact resistance between fibers within the composite bulk.

### Average Aspect Ratios

|                 | Stainless Steel | NiC |
|-----------------|-----------------|-----|
| As-Received     | 750             | 750 |
| Dry Blended     | 200             | 30  |
| Melt Compounded | 20              | 20  |

### Relative Morphologies

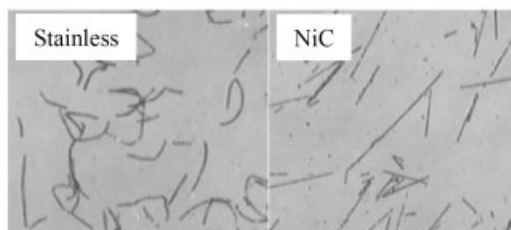
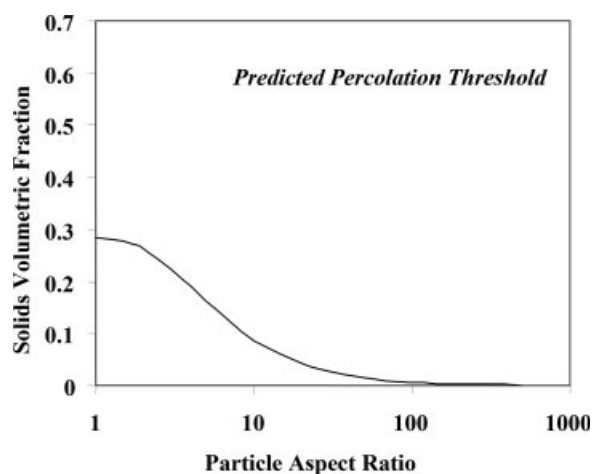
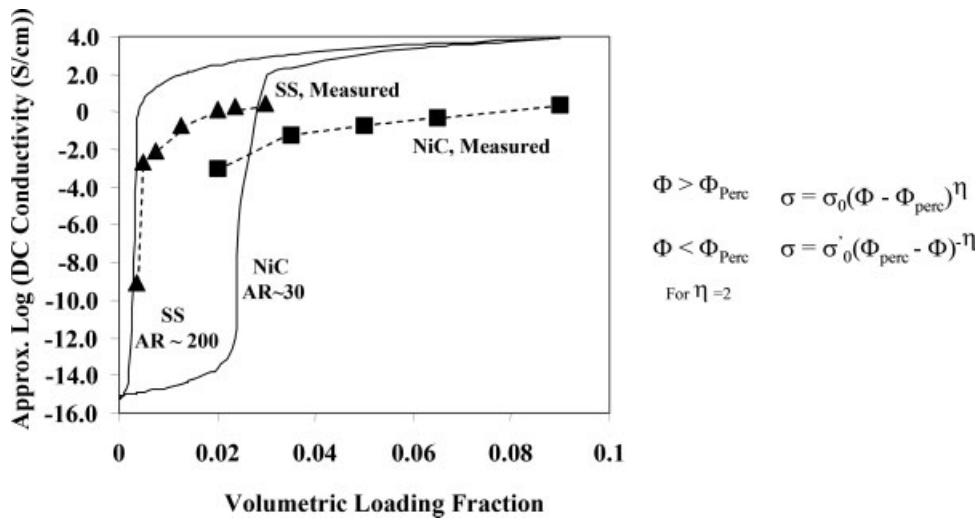


Figure 7 contrasts measured volumetric DC conductivity approximations of various polycarbonate and metal/metallized fiber combinations with the monocomponent stainless steel and NiC values shown in Figure 3.

Conductivity exhibits a plateau beyond the critical volume threshold due to the onset of a conductive path throughout the sample. Once established, increased filler loading does not significantly alter the measured value, ultimately limiting utility of conductivity as a characterization technique for shielding composites. As shown in Figure 8 shortcomings are apparent when considering that while a conductive path may exist between measurement electrodes, no assessment is made regarding homogeneity of fiber distribution throughout the molded



**Figure 5** Geometric percolation threshold versus loading levels as predicted by theory.<sup>29</sup> Lower amounts are required to achieve a conductive mixture as length to diameter ratio ( $L/D$ ) increases.



**Figure 6** Measured conductivity comparison of molded polycarbonate containing stainless steel and NiC fibers, and values predicted based upon percolation theory. Here,  $\Phi$  is loading level/concentration,  $\Phi_{Perc}$  is the percolation threshold (determined from aspect ratio and Figure 5),  $\sigma$  is composite electrical conductivity,  $\sigma_0$  is the intrinsic filler conductivity, and  $\eta$  is the so-called characteristic critical exponent<sup>26</sup> (assumed to be two for this example) describing the rapid variation of  $\sigma$  near the threshold concentration  $\Phi_{Perc}$ .

section. Figure 8 additionally illustrates that SE does not plateau with the increase in loading, but rather, continues to increase within the loading ranges typical to practical composite fabrication. Consequently, SE should be used as the primary characterization method.

Percolation concepts are then considered only a guide to minimum acceptable loadings in shielding applications; maximum packing fractions represent the upper bound on what filler volumes are required and are significantly larger than those required to achieve percolation. Figure 9 contrasts both quantities as a function of filler geometry. Superimposed are maximum packing fractions corresponding to the average aspect ratios measured in Figure 4 for both stainless steel and NiC. Large differences in required loadings result when L/D of either material is changed. Practical limits typically remain below the maximum packing values, because they can exceed levels, which can be readily injection molded into thin sections.

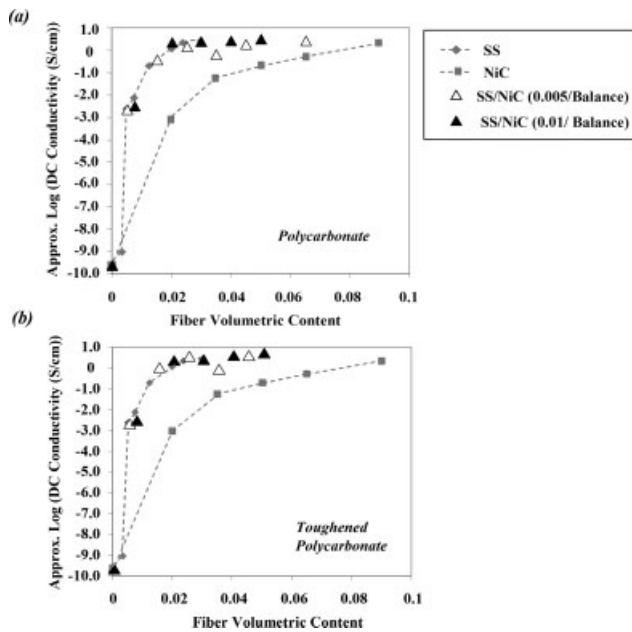


**Figure 7** Comparison of molded composite measured DC conductivity values for various polymer and fiber combinations with respect to fiber loading levels. (a) Unmodified PC and (b) Toughened PC. Background curves represent formulations with stainless steel or NiC fibers included as single fiber constituents.

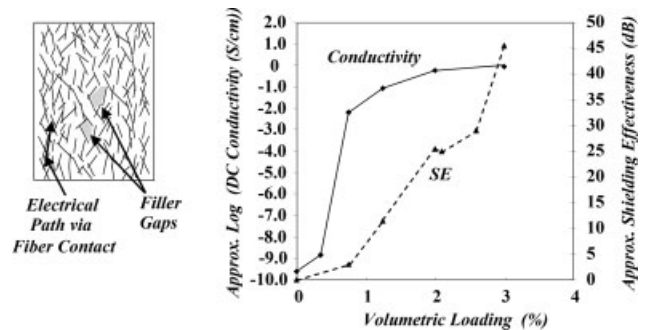


**Figure 8** DC volumetric conductivity measurements within filled composites reflect the conductive paths established within the molded specimen via entangled fiber, but not the potential for gaps within localized resin-rich regions. Plot contrasts molded DC conductivity values with SE determined via Stripline. Field methods<sup>22</sup> for ~ 2.66-mm thick stainless steel/polycarbonate composites.

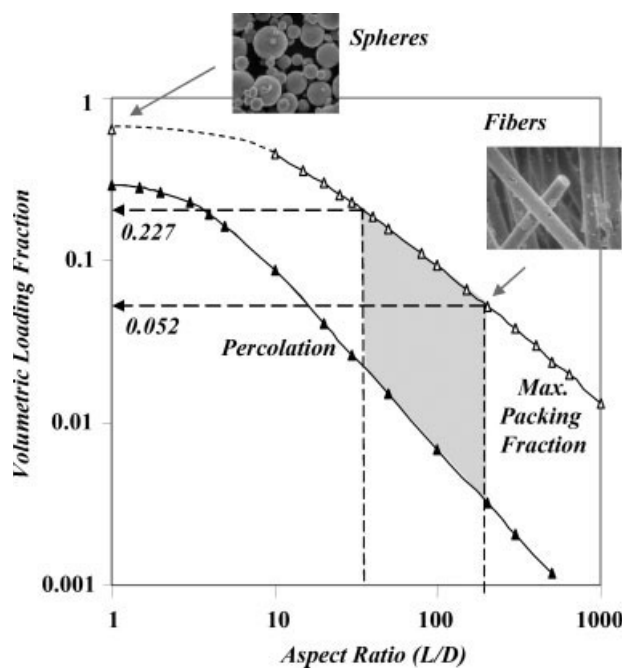
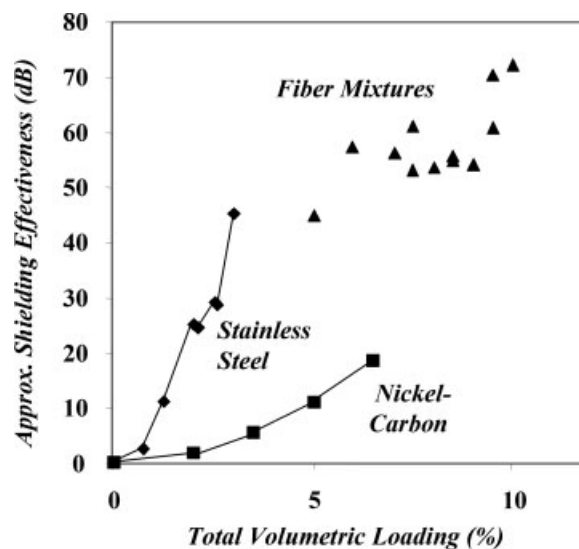


**Figure 9** Comparison of projected percolation values with maximum packing fractions as a function of filler L/D characteristics.<sup>26,29</sup> Dashed arrows correspond to approximate average aspect ratios measured in Figure 4 for both stainless steel ( $\sim 200$ ) and NiC ( $\sim 30$ ) following molding. Shaded region highlights the practical loading range.

The individual fiber types described in Figure 3 lead to differing shielding performances primarily due to their mechanical behavior during processing, as opposed to inherent conductivity differences between the stainless steel and metallic nickel constituents. The ductility of the stainless steel accommodates deformation induced by shear during polymer/carrier melting and subsequent flow into the cavity under pressure with minimal breakage.

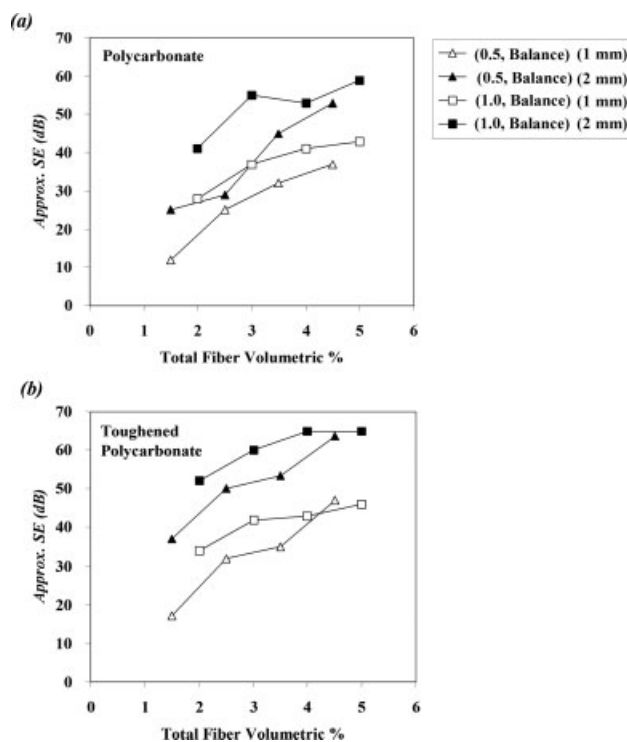
As a result, stainless steel is most efficient at network formation due to high overall aspect ratios as shown in Figure 10. This, however, leads to flow difficulties at higher loadings and limits overall shielding levels attainable within a practical thin-walled composite. Nickel-carbon is brittle, and fractures with shear, yielding low aspect ratios, and less efficient shielding. Although high loadings with NiC are easily achievable, material cost ultimately places limits on attainable shielding. Mixed fiber combinations with minor fractions of stainless steel take advantage of the deformable stainless component and shear-aligned nickel-carbon filaments, leading not only to easily moldable composites, but also to higher overall shielding formulations.

Figure 11 illustrates SE values measured through a range of loadings, wall thickness, and with various polymer matrix types. Shielding increases which result when changing from 1 to 2 mm wall thickness



**Figure 10** Shielding effectiveness versus volumetric loading of stainless steel and nickel carbon fibers. Shaded region/dashed curves represent mixtures of both components in various fractions, demonstrating dual-component advantages. Stripline Field measures,<sup>22</sup> data values at  $\sim 1$ –2 GHz,  $\sim 2.66$ -mm wall thickness.

range from  $\sim 10$  to 20 dB, which is consistent throughout loading ranges. Such relationships can be used as a guide for the selection of required fiber



**Figure 11** Average values of Shielding effectiveness (ASTM D 4935 measures<sup>21</sup>) versus volumetric loading for fiber mixtures within different matrix materials at varying thicknesses. Nomenclature: volume % (stainless steel, nickel carbon). (a) Polycarbonate (b) toughened polycarbonate.

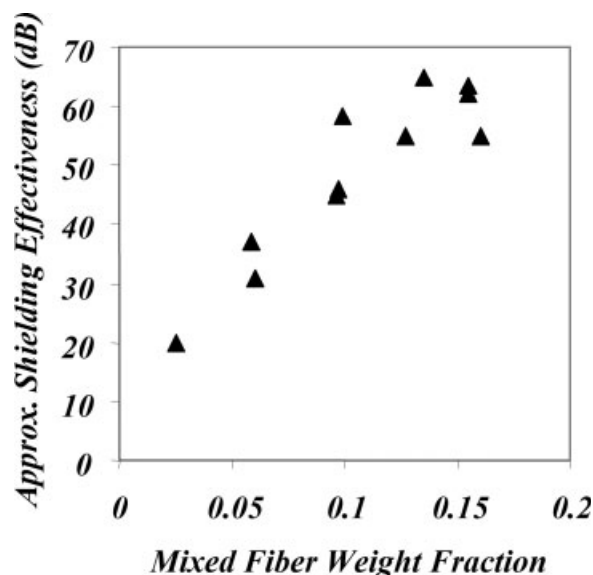


**Figure 12** Approximate/generalized relationship between shielding. Effectiveness and overall fiber fractional weight loading. Data representative of a range of filler levels within polycarbonate polymer matrix and additive types at 2-mm wall thickness.

volumetric loadings in conjunction with specification of the expected shielding requirements for a particular application. Figure 12 overlays shielding data for a variety of matrix materials, overall fiber fractional contents, and mixed fiber-type fractions, allowing an approximate relationship predicting effectiveness at particular weight contents to be developed.

### SUMMARY

ECP use within digital electronic applications requiring emission control has advantages in that it can be directly molded to a desired shape, serving to provide both the necessary shielding and mechanical integrity. Proper selection of base polymer, fiber types, content ratios, and wall thicknesses then enable production of easily formed articles, which can be readily designed for specific device operating characteristics to achieve a desired overall shielding response.

Metal and metallized fibers within conductive composites exhibit DC conductivity thresholds approximately equivalent to filler levels suggested by percolation theory based on particle aspect ratio, though measured magnitudes at higher loadings are lower than predicted values. Unlike DC conductivity, SE response does not exhibit a characteristic plateau behavior within loading ranges typical to practical use; volume fractions employed reside in the region above these thresholds, but below maximum geometric-packing fractions. Consequently, DC conductivity is of limited utility as an assessment measure for composite-shielding performance.

Shielding design practices within the industry consider specific IC clock frequencies and signal rise times as primary factors when assessing requirements for a given enclosure since they determine radiated emission characteristics. Apertures whose characteristic dimensions exceed  $\lambda/2$  provide no attenuation of emissions and a maximum  $\leq \lambda/20$  for this upper value should then be maintained; otherwise the inherent shielding capability of the enclosure material can cease to be a factor. Consequently, opening dimensions, wall thicknesses, and material shielding behavior all combine to have bearing on formulation selection.

SE of polycarbonate-based formulations can attain average levels of  $\sim 50$ – $60$  dB through 2 GHz at 2 mm thickness as measured by ASTM D 4935. These values vary with wall thickness; improvements which result when increasing from 1 to 2 mm typically range  $\sim 10$ – $20$  dB.

These compositional and electrical characteristics combine to form the basis for practical relationships between enclosure requirements and molded polymer composite properties and can then be used as a guide for material formulation selection and use.

The authors acknowledge Susan Babinec, Ludo Aerts, Mike Hus, Mike Malanga, and Tom Tarnowski of The Dow Chemical Company.

### References

1. Bigg, D. M.; Stutz, D. E. *Polym Compos* 1983, 4, 40.
2. Krueger, Q.; King, J. *Adv Polym Technol* 2003, 22, 96.
3. Clingerman, M.; Weber, E.; King, J.; Schulz, K. *Polym Compos* 2002, 22, 911.
4. Chen, S. C.; Chien, R. D.; Lee, P. H.; Huang, J. S. *J Appl Polym Sci* 2005, 98, 1072.
5. Chou, K. S.; Huang, K. C.; Shih, Z. H. *J Appl Polym Sci* 2005, 97, 128.
6. Fox, R.; Babinec, S.; Howard, K.; Chartier, M.; Clarey, T.; Peters, R. E. U.S. Pat. 6,936,191 B2 (1995).
7. Fox, R.; Wani, V.; Hus, M. U.S. Pat. 6,896,828 B2 (1995).
8. Barnes, J. R. *Electronic System Design: Interference and Noise Control Techniques*; Prentice-Hall: New Jersey, 1987.
9. Neo, C. P.; Varadan, V. K. *IEEE Trans Electromagn Comp* 2004, 46, 102.
10. Hanada, E.; Takano, K.; Antoku, Y.; Matsumura, K.; Hoshino, Y.; Nishimura, T.; Hyoudou, K.; Watanabe, Y.; Nose, Y. *IEEE EMC Newslett* 2003.
11. Ott, H. W. *Noise Reduction Techniques in Electronic Systems*; Wiley: New York, 1976.
12. White, D. R. J. *Shielding Design Methodology and Procedures: Interference Control Technologies*; Gainesville, VA, 1986.
13. White, D.; Mardiguian, M. *Electromagnetic Shielding, Vol.3: EMF-EMI Control*; Gainesville, VA, 1988.
14. Kimmel, W. *Designing for EMC*; Kimmel Gerke Assoc Ltd: St. Paul, MN, 2001.
15. Archambeault, B. *PCB Design for Real-World EMI Control*; Kluwer: Norwell, MA, 2002.
16. Montrose, M. *Printed Circuit Board Design Techniques for EMC Compliance: A Handbook for Designers*, 2nd ed.; IEEE Press: New York, 2000.



17. Paul, C. R. *Introduction to Electromagnetic Compatibility*; Wiley: New York, 1992.
18. The Dow Chemical Company, Midland, MI.
19. Bekaert Fibre Technologies, 12 T.W. Alexander Drive, PO Box 1359, Research Triangle Park, NC.
20. Novamet Specialty Products Corp., 681 Lawlins Road, Wyckoff, NJ.
21. American Society for Testing and Materials; ASTM D 4935-99; Philadelphia PA, 1999.
22. Kempel, L. C.; Rothwell, E. J.; Wilmhoff, B.; Nyquist, D.; Howard, K. Twenty-Third AMTA Mtg and Symposium, Boulder, CO, 2001.
23. Bigg, D. M. *Metal Filled Polymers Properties and Applications*; Bhattacharya, S. K. Ed.; Marcel Dekker; New York, 1986; Chapter 3.
24. Milewski, J. J. *Ind Chem Prod Res Dev* 1978, 17, 363.
25. Bigalke, J. *Phys A* 1999, 272, 281.
26. Garboczi, E. J.; Zinder, K. A.; Douglas, J. F. *Phys Rev E* 1995, 52, 819.
27. Bergman, D. *Phys A* 1989, 157, 72.
28. Harris A.; Lubensky, T. *Phys Rev B* 1987, 35, 6964.
29. Bicerano, J.; Douglas, J. F.; Brune, D. A. *J Macromol Sci Rev* 1999, C 39, 561.